4. J.H. Chou, J.F. Chang, D.B. Lin, H.J. Li, and T.L. Wu, A compact loop-slot mode combination antenna for ultra-thin tablet computer with metallic bottom cover, IEEE Antennas Wireless Propag Lett 13 (2014), 746–749.
5. Laser direct structuring, LPKF Laser & Electronics AG, Available at http://www.lpkf.com/applications/mid/index.htm.
6. Ansoft Corporation HFSS, Available at: http://www.ansoft.com/products/hf/hfss.
7. SG 64, SATIMO, Available at: http://www.satimo.com/content/products/sg-64.
8. S.W. Su, A. Chen, and L. Tai, Compact patch antenna mountable above conducting plate for WLAN operation, Electron Lett 42 (2006), 1130–1136.
9. C.T. Lee and S.W. Su, Tri-band, stand-alone, PIFA with parasitic, inverted-L plate and vertical ground wall for WLAN applications, Microwave Opt Technol Lett 53 (2011), 1797–1803.
10. J.L. Volakis, Antenna engineering handbook, 4th ed., Chapter 6, McGraw-Hill, New York, 2007, pp. 16–19.
11. C.A. Balanis, Antenna theory: analysis and design, 3rd ed., Chapter 2, Wiley, Hoboken, NJ, 2012.

GAIN ENHANCEMENT OF THE VIVALDI ANTENNA WITH BAND NOTCH CHARACTERISTICS USING ZERO-INDEX METAMATERIAL

Manoj Bhaskar, Esha Johari, Zubair Akhter, and M. J. Akhtar
Department of Electrical Engineering, Indian Institute of Technology, Kanpur, Uttar Pradesh, 208016, India; Corresponding author: zuakhter@iitk.ac.in

Received 30 May 2015

ABSTRACT: *In this letter, a tapered slot ultrawide band (UWB) Vivaldi antenna with enhanced gain having band notch characteristics in the WLAN/WiMAX band is presented. In this framework, a reference tapered slot Vivaldi antenna is first designed for UWB operation that is, 3.1–10.6 GHz using the standard procedure. The band-notch operation at 4.8 GHz is achieved with the help of especially designed complementary split ring resonator (CSRR) cell placed near the excitation point of the antenna. Further, the gain of the designed antenna is enhanced substantially with the help of anisotropic zero index metamaterial (AZIM) cells, which are optimized and positioned on the substrate in a particular fashion. In order to check the novelty of the design procedure, three distinct Vivaldi structures are fabricated and tested. Experimental data show quite good agreement with the simulated results. As the proposed antenna can minimize the electromagnetic interference (EMI) caused by the IEEE 802.11 WLAN/WiMAX standards, it can be used more efficiently in the UWB frequency band.* © 2016 Wiley Periodicals, Inc. Microwave Opt Technol Lett 58:233–238, 2016; View this article online at wileyonlinelibrary.com. DOI 10.1002/mop.29534

Key words: *anisotropic zero index metamaterial; complementary split ring resonator; Vivaldi antenna*

1. INTRODUCTION

In recent years, there is a lot of interest to integrate various types of metamaterial unit cells with the tapered slot Vivaldi antenna (TSVA) to improve the overall radiation characteristics [1–4]. The Vivaldi antennas are already well known for their UWB characteristics which can be further improved using extended ground plane stubs [5]. However, the main limitation of the Vivaldi antenna has been its low directivity [6,7]. In the past, researchers have proposed several methods such as the array structure [8], the photonic band gap (PBG) structure [9], and the double slot structure in order to improve its directivity [10]. Most of these methods, however, increase the complexity and overall cost of the resultant system.

A number of Vivaldi antennas having various configurations have been proposed in literature for various applications such as GPR [11], cancer detection [12], and UWB communication [13]. One of the challenges of the UWB communication band has been the electromagnetic interference (EMI) caused due to WiMAX and WLAN applications. It has been reported that loading of the Vivaldi antenna with SRR (Split Ring Resonator) structure has the potential to reduce the interference caused due to WiMAX and WLAN signals [14]. However, the SRR loading also deteriorates the overall gain of the antenna especially at the resonating frequency corresponding to the SRR structure. Hence, reduction of the overall gain of the Vivaldi antenna is one of the major issues while using a SRR structure to provide the band notch characteristics at certain frequency bands.

In this letter, a special type of anisotropic zero index metamaterial (AZIM) unit cell is designed and loaded along the aperture of the band-notched Vivaldi antenna to improve its overall gain. The complementary split ring resonator (CSRR) introduced

TABLE 1 Optimized Parameters for Reference TSVA

Parameters	L	L_1	L_2	W_0	W	W_1	W_2	R_s	R_c	α
Value (in mm)	50	5	2	0.5	50	1.11	0.4	5.3	3.7	70^0

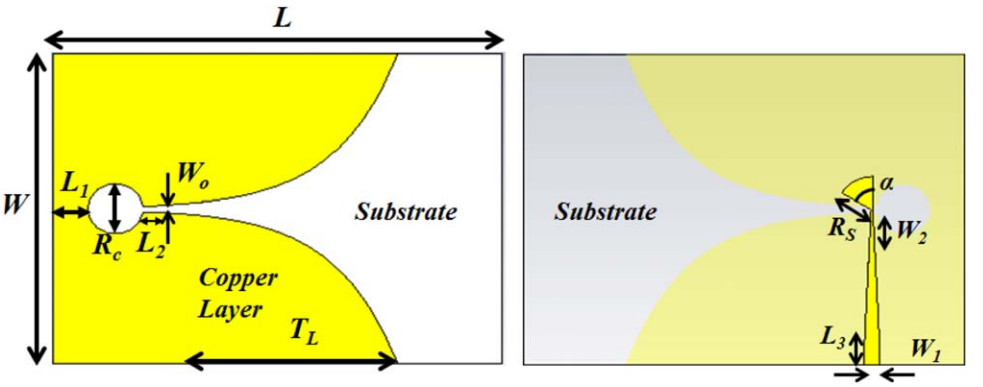

Figure 1 Simulated reference Vivaldi Antenna (a) top and (b) bottom view. [Color figure can be viewed in the online issue, which is available at wileyonlinelibrary.com]

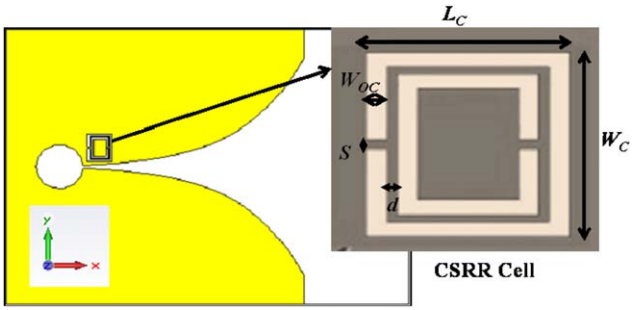

Figure 2 The tapered slot Vivaldi antenna loaded with the CSRR cell along with its zoomed dimensions: $L_c = 4$ mm, $W_c = 5.1$ mm, $d = 0.2$ mm, $s = 0.3$ mm, $W_{oc} = 0.4$ mm. [Color figure can be viewed in the online issue, which is available at wileyonlinelibrary.com]

near the feed point of the antenna facilitates a band notch operation for rejecting the unwanted (WiMAX, WLAN) signals. The resonance frequency of the CSRR cell can be tuned to the desired frequency by optimizing the dimensions of the cell. The proposed antenna shows good UWB communication properties in the entire operating band (3.1–10.6 GHz) with the enhanced gain characteristics and the band notch frequency of 4.8 GHz.

2. TAPERED SLOT VIVALDI ANTENNA DESIGN

The reference Vivaldi antenna is designed using the FR-4 substrate ($\varepsilon_r = 4.3$, tan $\delta = 0.025$) with thickness of 0.8 mm. The initial parameters of the reference antenna are obtained using the basic design equations given in [6,7]. The final design parameters of the proposed antenna are obtained after optimizing them with the help of the 3D electromagnetic solver, the CST Studio as shown in Table 1. The top and bottom layout for the designed TSVA with all the antenna design parameters are shown in Figure 1.The excitation outline of the antenna is described in Figure 1(b) where W_1 and W_2 are the optimized microstrip line widths in order to provide good matching conditions.

3. COMPLEMENTARY SPLIT RING RESONATOR

The initially proposed metamaterial resonator was the edge coupled split ring resonator (SRR) having negative

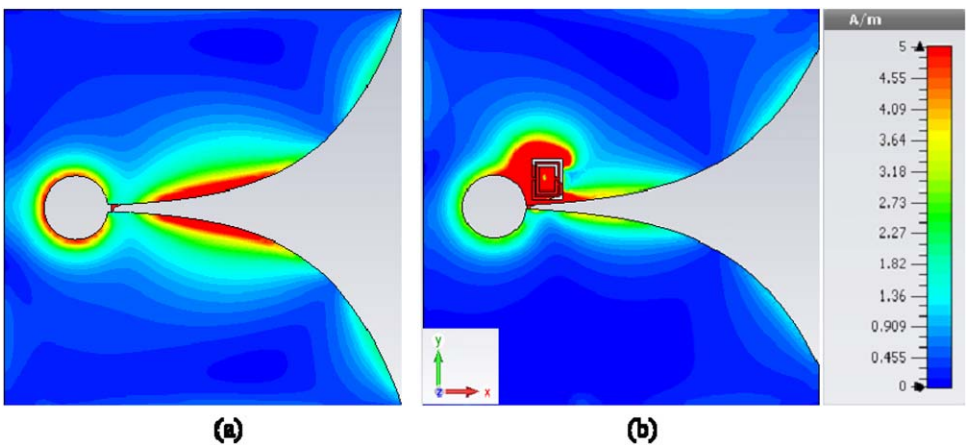

Figure 3 Absolute value of current distribution for (a) reference TSVA, (b) CSRR loaded TSVA. [Color figure can be viewed in the online issue, which is available at wileyonlinelibrary.com]

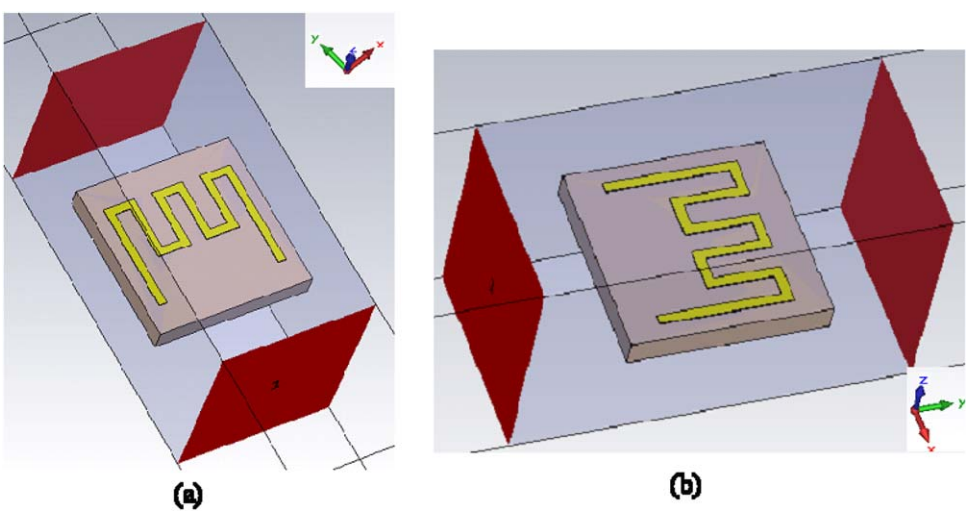

Figure 4 Simulation setup of AZIM unit cell. [Color figure can be viewed in the online issue, which is available at wileyonlinelibrary.com]

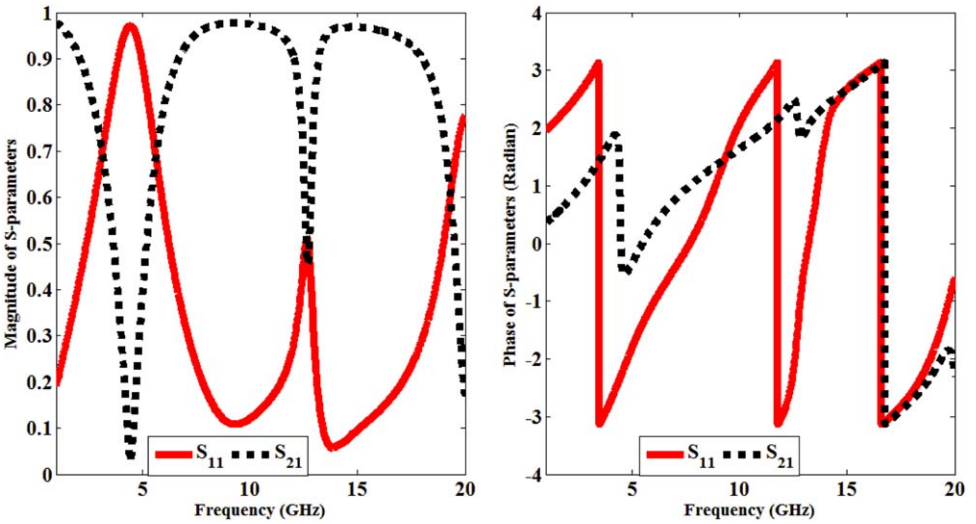

Figure 5 Linear magnitude and phase plot of scattering parameters of the AZIM unit cell. [Color figure can be viewed in the online issue, which is available at wileyonlinelibrary.com]

permeability [15]. The conventional SRR was later on modified into the CSRR by applying Babinet's principle in order to have more flexibility in design [16]. In this work, the CSRR configuration is used for the band notch application with the unit cell shown in Figure 2. The CSRR unit cell is positioned near to the feed point in order to excite it with the normal electric field component. The position of the proposed CSRR unit cell is optimized in order to achieve the substantial amount of signal rejection as shown in Figure 2.

The effect of CSRR loading on the Vivaldi antenna is shown by the current distribution in Figure 3 at resonant frequency of 4.8GHz. It is clear from this figure that at the resonant frequency of CSRR cell, the current distribution on the surface of TSVA is minimum, which basically means that the antenna is not radiating at 4.8 GHz.

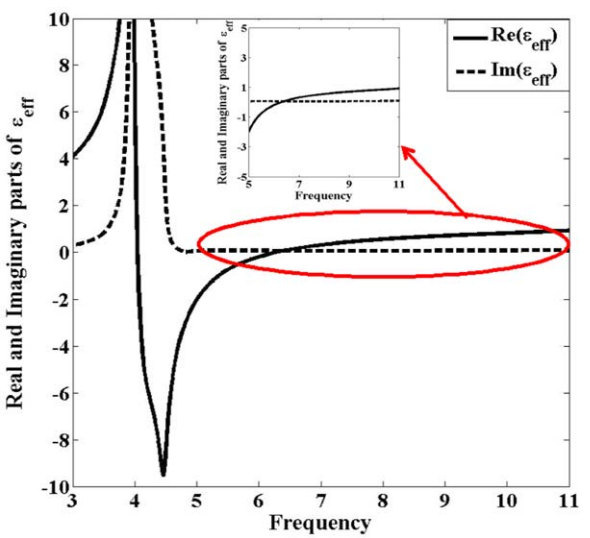

Figure 6 AZIM unit cell permittivity variation with the frequency. [Color figure can be viewed in the online issue, which is available at wileyonlinelibrary.com]

4. ANISOTROPIC ZERO INDEX METAMATERIAL CELL

The loading of AZIM unit cells to the reference TSVA enhances the directivity of the CSRR loaded Vivaldi antenna. The dimensions of the AZIM cell are optimized with the help of CST EM simulator as shown in Figure 4 to obtain the desired characteristics. The reflection and transmission characteristics of the optimized AZIM cell in the given frequency band are shown in Figure 5. The effective relative permittivity of proposed AZIM cell along the direction of beam radiation is calculated using a MATLAB program based on the standard retrieval procedure [17] as presented in Figure 6. It can be observed from this plot that the proposed AZIM cell is operating quite efficiently in the higher frequency band as the effective relative permittivity is near to zero in the frequency range of 6–10.6 GHz.

The placement of AZIM cells on tapered section of antenna is done as shown in Figure 7. The feed line position and other dimensions of the TSVA remain unchanged after insertion of AZIM cells to the structure.

A comparison of the near electric field distribution for the reference TSVA, and for the TSVA implanted with the AZIM cells is shown in Figure 8. It can be observed from Figures 8(a) and (b) that the AZIM cells modify the near field phase fronts and produces some focusing effects so that a plane wave approximation can be assumed quite near to the antenna than otherwise [18].

5. ANTENNA MEASUREMNETS AND RESULTS

The proposed Vivaldi antenna along with the designed CSRR and AZIM cells was fabricated and tested for operation in the frequency range of 3.1–10.6 GHz as shown in Figure 9.

5.1. Voltage Standing Wave Ratio Measurement

The return loss and VSWR measurements were done using the Agilent PNA N5230C Network Analyzer. The simulated and measured VSWR plots for the reference antenna, the antenna loaded with the CSRR cell, and the antenna with both CSRR and AZIM cells are shown in Figure 8. The addition of CSRR cell to the reference TSVA exhibits narrow band rejection at the center frequency of 4.8 GHz with VSWR > 2 around this frequency.

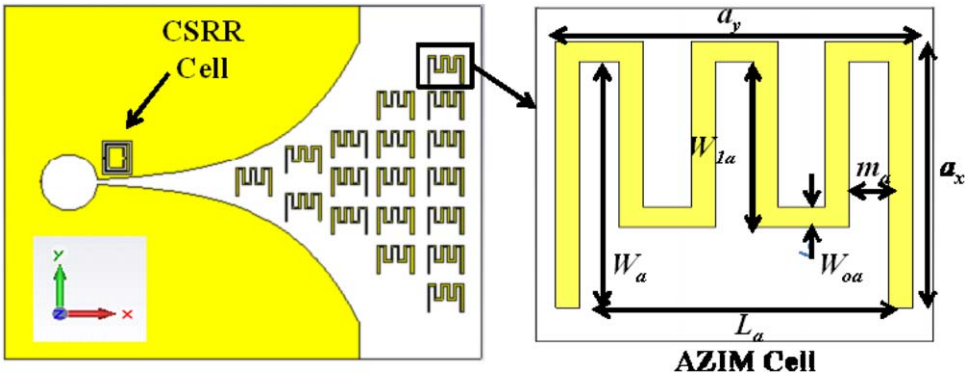

Figure 7 AZIM and CSRR Loaded TSVA with zoomed view of square AZIM cell: $a_x = a_y = 6$ mm, $W_a = 5$ mm, $W_{1a} = 2.5$ mm, $W_{oa} = 0.3$ mm, $m_a = 0.5$ mm and $L_a = 5$mm. [Color figure can be viewed in the online issue, which is available at wileyonlinelibrary.com]

The loading of AZIM cells to the CSRR loaded TSVA is a critical task as it might affect the impedance matching of the TSVA. However, in the present design, the dimensions and position of the AZIM cells are properly optimized such that the VSWR is not significantly changed after their insertion as can be seen from Figure 10.

5.2. Radiation Pattern Measurement

The measurement of all the designed antennas has been carried out in the anechoic environment as shown in Figure 11. The Ridged horn antenna is taken as the reference receiving antenna. The effect of AZIM cells on designed antennas for directivity enhancement can be easily observed from the radiation pattern plots as shown in Figure 12. The beamwidth of AZIM cells loaded antenna is decreased significantly as compared to the reference TSVA. A comparison of peak realized gain for the reference TSVA and the proposed antenna (CSRR and AZIM loaded) has also been demonstrated in Figure 13.

From measured gain as shown in Figure 11 it can be observed that the maximum gain is enhanced by 2.6 dBi in the frequency range of 5.8–8.5 GHz relative to the unloaded reference TSVA. The gain enhancement is more pronounced in the higher frequency band due to the designed AZIM characteristics for high frequency operation as shown in Figure 6.

6. CONCLUSION

In this letter, a modified tapered slot Vivaldi antenna with integrated AZIM and CSRR cells has been proposed to improve the overall radiation characteristics of the reference antenna. Initially, the CSRR unit cell has been used to achieve the band-notch operation at 4.8 GHz of the UWB Vivaldi antenna. This results into the gain distortion of the antenna particularly at the CSRR resonating frequency. In the next step, the AZIM cells have been incorporated into the CSRR loaded Vivaldi antenna which resulted into enhancement of the peak realized gain by 2.6 dBi especially at higher frequencies. The antennas have been fabricated and tested to validate the proposed design. The proposed Vivaldi antenna has good potential for UWB communication applications with the enhanced gain, and reduced EMI from WLAN, WIMAX standards.

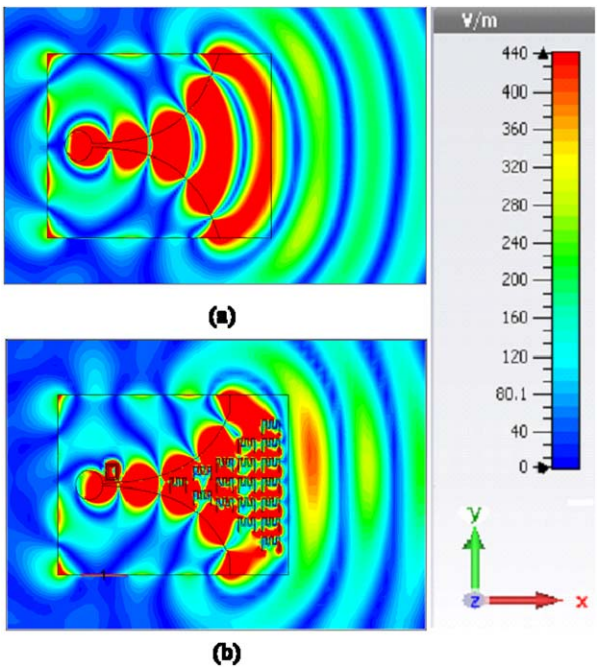

Figure 8 Field distribution for (a) reference TSVA and (b) AZIM cells loaded TSVA at 10 GHz. [Color figure can be viewed in the online issue, which is available at wileyonlinelibrary.com]

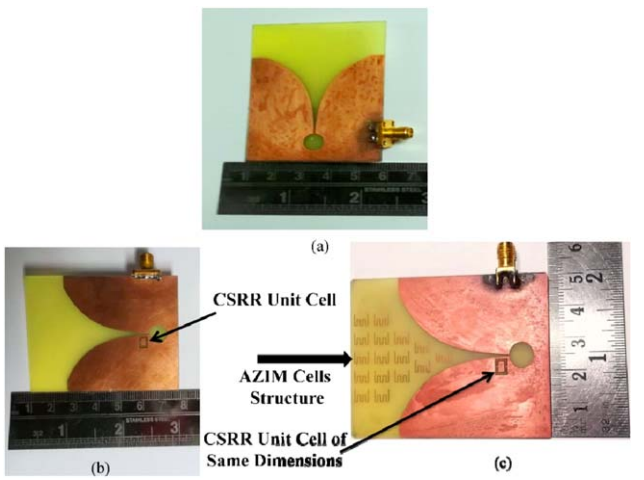

Figure 9 Fabricated antennas (a) reference TSVA, (b) CSRR loaded TSVA, and (c) AZIM and CSRR loaded TSVA. [Color figure can be viewed in the online issue, which is available at wileyonlinelibrary.com]

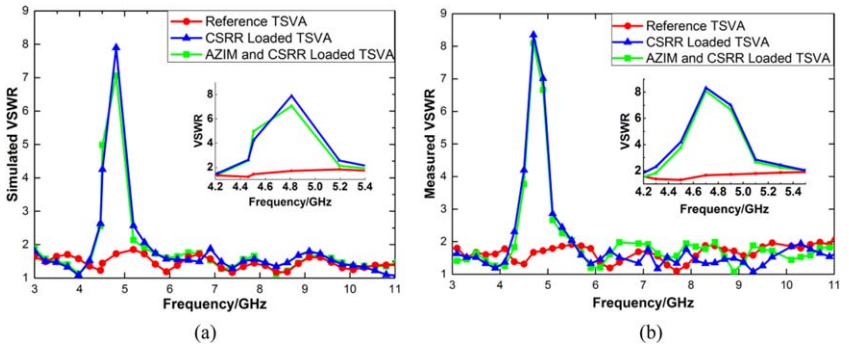

Figure 10 VSWR plots for all three designed antennas: (a) simulated and (b) measured. [Color figure can be viewed in the online issue, which is available at wileyonlinelibrary.com]

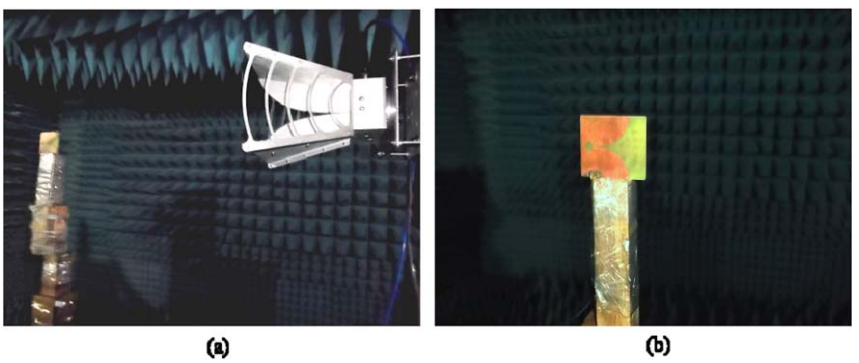

Figure 11 Antenna measurement setup in Anechoic Chamber for (a) reference TSVA and (b) AZIM and CSRR loaded TSVA. [Color figure can be viewed in the online issue, which is available at wileyonlinelibrary.com]

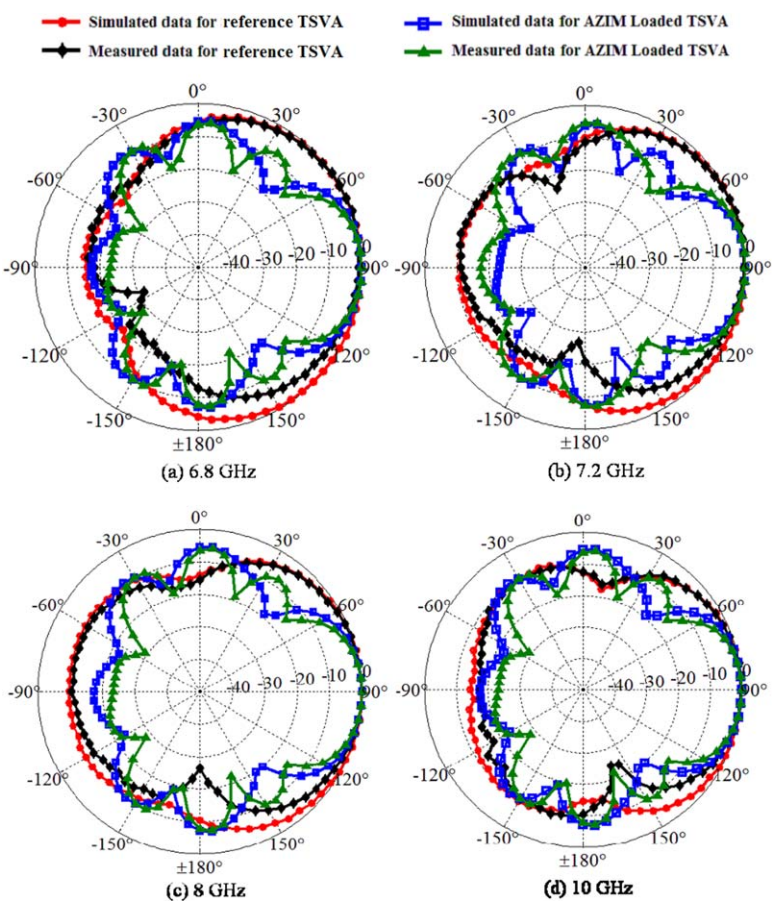

Figure 12 Radiation pattern plots obtained in anechoic chamber for designed antennas. [Color figure can be viewed in the online issue, which is available at wileyonlinelibrary.com]

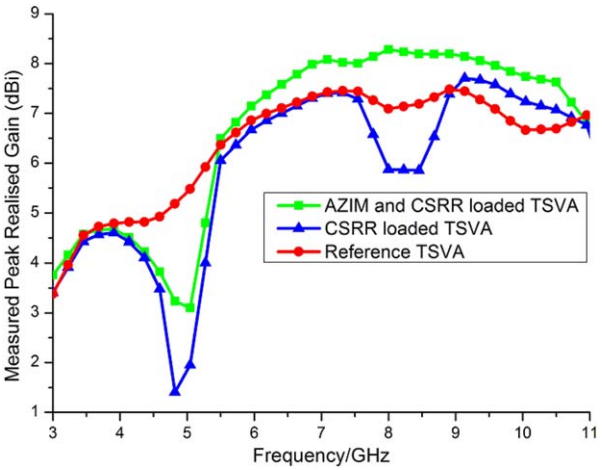

Figure 13 Measured peak realized gain for all three designed antennas. [Color figure can be viewed in the online issue, which is available at wileyonlinelibrary.com]

REFERENCES

1. B. Zhou and T.J. Cui, Directivity enhancement to Vivaldi antennas using compactly anisotropic zero-index metamaterials, IEEE Antennas Wireless Propag Lett 10 (2011), 326–329.
2. K. Li, C. Zhu, L. Li, Y.-M. Cai, and C.-H. Liang, Design of electrically small metamaterial antenna with ELC and EBG loading, IEEE Antennas Wireless Propag Lett 12 (2013) 678–681.
3. M. Sun, Z.N. Chen, and X. Qing, Gain enhancement of 60-GHz antipodal tapered slot antenna using zero-index metamaterial, IEEE Trans Antennas Propag 61 (2013), 1741–1746.
4. M. Bhaskar, Z. Akhter, S.L. Gupta, and M.J. Akhtar, Design of anisotropic zero-index metamaterial loaded tapered slot Vivaldi antenna for microwave imaging, In: IEEE Antennas and Propagation Society International Symposium 2014, Memphis, TN, pp. 1594–1595.
5. J. Wu, Z. Zhao, and Q.H. Liu, A novel Vivaldi antenna with extended ground plane stubs for ultra-wideband applications, Microwave Optical Tech Lett 57 (2015).
6. P. Piksa and V. Sokol, Small Vivaldi antenna for UWB, In: Proceedings of the Conference RADIOELEKTRONIKA, 2005, pp. 490–493.
7. P.J. Gibson, The Vivaldi aerial, In: 9th European Microwave Conference, 1979, pp. 101–105.
8. E.W. Reid, L. Ortiz-Balbuena, A. Ghadiri, and K. Moez, A 324-element Vivaldi antenna array for radio astronomy instrumentation, IEEE Trans Antennas Propag 61 (2012), 241–249.
9. T.J. Ellis and G.M. Rebeiz, MM-wave tapered slot antennas on micro machined photonic band gap dielectrics, In: IEEE MTT-S International Microwave Symposium Digest, 2 (1996), 1157–1160.
10. Y.W. Wang, G.M. Wang, and B.F. Zong, Directivity improvement of Vivaldi antenna using double-slot structure, IEEE Antennas Wireless Propag Lett 12 (2013), 1380–1383.
11. M.D. Elsheakh and E.A. Abdallah, Compact shape of vivaldi antenna for water detection using Ground pentrating radar, Microwave Optical Tech Lett 56 (2014).
12. A. Lazaro, R. Villarino, and D. Girbau, Design of tapered slot vivaldi antenna for UWB breast cancer detection, Microwave Optical Tech. Lett 53 (2011).
13. R. Natarajan, J. George, M. Kanagasabai, and S. Arunkumar, A compact antipodal Vivaldi Antenna for UWB applications, IEEE Antennas Wireless Propag Lett 99 (2015), 1.
14. X. Liu, Z. Lei, R. Yang, J. Zhang, L. Chen, and X. Kong, The band notch sensitivity of Vivaldi antenna towards CSRRs, Prog Electromagn Res Lett 43 (2013), 125–135.
15. B. Pendry, A. John, J. Holden, D.J. Robbins, and W.J. Stewart, Magnetism from conductors and enhanced nonlinear phenomena, IEEE Trans Microwave Theory Tech 47 (1999), 2075–2084.
16. F. Falcone, T. Lopetegi, J.D. Baena, R. Marqu, F. Martin, and M. Sorolla, Effective negative-ε stop-band microstrip lines based on complementary split ring resonators, IEEE Microwave Wireless Compon Lett 2004 (14), 280–282.
17. R. Smith, S. Schultz, P. Markos, and C.M. Soukoulis, Determination of effective permittivity and permeability of metamaterials from reflection and transmission coefficients, Phys Rev B 65 (2002), 195104.
18. D.M. Pozar, Microwave engineering, 3rd ed., Wiley, Hoboken, NJ, 1997.

WIDEBAND COMPACT 2D PHOTONIC CRYSTAL SWITCH BASED ON FERRITE RESONATOR IN SQUARE LATTICE WITH 90° BENDING

Victor Dmitriev, Daimam Zimmer, and Gianni Portela
Department of Electrical Engineering, Federal University of Para, Av. Augusto Correa 01, Belem, Para, 66075-900, Brazil

Received 5 June 2015

ABSTRACT: *We suggest and analyse theoretically a wideband switch with a very simple and compact structure. It consists of a 90°-waveguide bending in a photonic crystal with square unit cell and a circular ferrite cylinder placed in the bending. The state OFF of the switch corresponds to the nonmagnetized ferrite. The structure of the standing wave in the input waveguide with a node oriented along the output waveguide prevents excitation of the output waveguide. In the state ON, different resonant modes of the magnetized ferrite resonator provide high transmission from input port to output one, namely, both clockwise and anticlockwise dipole rotating modes, the standing dipole mode which is the sum of the two rotating modes and also a travelling wave. Our numerical simulations show that in the subterahertz region, the switch possesses the frequency band of 8% at the levels of insertion losses lower than −2 dB and isolation better than −22 dB. This bandwidth is one order of magnitude higher than that reported in the literature for switches of this type.* © 2016 Wiley Periodicals, Inc. Microwave Opt Technol Lett 58:238–242, 2016; View this article online at wileyonlinelibrary.com. DOI 10.1002/mop.29537

Key words: *switching; photonic crystals; ferrite resonators*

1. INTRODUCTION

Switches are essential elements of communication networks. To control light in photonic crystal (PhC) circuits, different methods can be used. Switches and modulators based on control of light by light, by electric field, by heat or by DC magnetic field have been suggested recently [1–4]. In particular, changing some parameters of magneto-optical (MO) waveguide [4] and resonators [5] by a DC magnetic field $\mathbf{H}_0$, one can control the flow of electromagnetic waves in communication systems.

In our previous article [6,7], we suggested two-dimensional (2D) PhC switches based on MO resonator and discussed two possible mechanisms of switching. In nonmagnetized ferrite resonator, the mechanism is based on a standing mode (usually dipole one). In the magnetized ferrite resonator, one of the possible mechanisms is based on the standing wave in the MO resonator, and the second mechanism is stipulated by clockwise or anticlockwise rotating dipole mode.

The bandwidth of the switches discussed in [6,7] depends on many factors. Among others, the bandwidth is defined by mechanism of switching, that is, by the type of resonator modes (standing or rotating) involved in the switching process. Besides,